

Optical Engineering

SPIEDigitalLibrary.org/oe

Length distributed measurement of temperature effects in Yb-doped fibers during pumping

Martin Leich
Julia Fiebrandt
Anka Schwuchow
Sylvia Jetschke
Sonja Unger
Matthias Jäger
Manfred Rothhardt
Hartmut Bartelt



Length distributed measurement of temperature effects in Yb-doped fibers during pumping

Martin Leich,* Julia Fiebrandt, Anka Schwuchow, Sylvia Jetschke, Sonja Unger, Matthias Jäger, Manfred Rothhardt, and Hartmut Bartelt

Leibniz Institute of Photonic Technology, Albert-Einstein-Str. 9, 07745 Jena, Germany

Abstract. We demonstrate a distributed measurement technique to observe temperature changes along pumped Yb-doped fibers. This technique is based on an array of fiber Bragg gratings acting as a temperature sensor line. The Bragg gratings are inscribed directly into the Yb-doped fiber core using high-intensity ultrashort laser pulses and an interferometric setup. We studied the temperature evolution in differently co-doped Yb fibers during optical pumping and identified different effects contributing to the observed temperature increase. We found that preloading of fibers with hydrogen supports the formation of Yb²⁺ during UV irradiation and has a large impact on fiber temperature during pumping. The proposed technique can be applied to investigate the homogeneity of pump absorption in active fibers and to support spatially resolved photodarkening measurements. © The Authors. Published by SPIE under a Creative Commons Attribution 3.0 Unported License. Distribution or reproduction of this work in whole or in part requires full attribution of the original publication, including its DOI. [DOI: 10.1117/1.OE.53.6.066101]

Keywords: fiber Bragg grating; temperature sensing; rare-earth-doped fibers; optical pumping; photodarkening.

Paper 140445P received Mar. 18, 2014; revised manuscript received May 9, 2014; accepted for publication May 13, 2014; published online Jun. 3, 2014.

1 Introduction

Since fiber lasers and amplifiers have been scaled up to the kW-level,¹ they have attracted much attention in science and industry. According to the fiber laser application, different resonator types have evolved, utilizing different kinds of fibers, and reflecting elements for the resonator design. A promising concept to realize efficient and power stable monolithic fiber laser systems is the use of short fibers with high concentrations of active ions and large mode areas implementing the high reflecting optical elements, which define the resonator, directly inside the active fiber, e.g., as fiber Bragg grating (FBG).

The fabrication of FBGs was first demonstrated by Hill et al.² The development of holographic inscription techniques³ enables the realization of Bragg grating periods and therewith Bragg reflection wavelengths nearly independent of the laser source. Nevertheless, the photosensitivity of the fiber material to the inscription laser radiation and the wavelength-dependent diffraction limit have to be considered for FBG fabrication.

Commonly employed laser sources in holographic inscription setups are excimer and exciplex lasers emitting UV nanosecond pulses. With such sources, FBGs in UV-photosensitive but mostly passive fibers have been realized, e.g., in Ge-doped (standard) fibers applied for temperature and strain sensing. The photosensitivity is even high enough to produce single-pulse FBGs using UV ns pulses, therewith allowing a very efficient draw-tower grating production.⁴ To apply techniques utilizing UV ns pulses for inscription to active, i.e., rare-earth-doped fibers, they have to be sensitized by a germanium or boron co-doping⁵ during preform fabrication and/or by hydrogen loading⁶ prior to grating inscription. With the development of femtosecond solid state laser

sources, a material-independent laser microstructuring was possible allowing direct FBG inscription into actively doped fibers without the need for presensitization. Due to the high intensities available with femtosecond-pulse laser systems, the optical band gap could be overcome by nonlinear absorption processes,⁷ producing index changes required for FBG inscription. Even a five-photon-absorption is possible [at 800 nm (Ref. 8)]; while using ns pulse sources only one- or two-photon absorption takes place.⁹

Although fiber lasers with UV ns pulse-inscribed FBGs in photosensitized fibers⁶ have also been demonstrated, the first laser operating in pure Yb-doped aluminosilicate fibers was reported in Ref. 10 using 800-nm fs pulses and a phase mask technique for FBG inscription. Further on, various inscription wavelengths [400 nm (Ref. 11) and 266 nm (Ref. 12)] and techniques (point-by-point inscription¹³ and two-beam interferometry¹²) have been established.

In addition to FBG fabrication, an important issue in realizing monolithic fiber lasers is the thermal and power stability of the cavity. Especially, the knowledge of temperature effects in rare-earth-doped fibers is of great interest in order to improve the performance and stability of monolithic fiber lasers and fiber amplifiers, because heat load and scattering within the fiber core during optical pumping can cause destruction of the coating or the fiber itself. Moreover, a temperature increase in Yb-doped fibers results in a change of essential material parameters, e.g., the reduction of fluorescence lifetime and absorption cross section of Yb³⁺.¹⁴ Also, the photodarkening (PD) kinetics are strongly influenced by temperature changes,¹⁵ and PD measurement results may be misinterpreted if the fiber temperature is not considered during measurement.

Absorbing defects generated during FBG inscription need to be considered as well. It has already been demonstrated that a temperature treatment of type II FBGs written with 800-nm fs pulses¹⁶ and type I FBGs fabricated with 266-nm fs pulses¹⁷ can remove the heat-causing absorption

*Address all correspondence to: Martin Leich, E-mail: martin.leich@ipht-jena.de

through FBG-inscription and in the latter case¹⁷ can improve the spectral shape of the laser emission. Another possibility to remove UV-induced losses is a subsequent low-power UV photobleaching¹⁸ treatment, where the density of absorbing species can be reduced based on the existence of loss equilibrium states.

Within this report, we now utilize FBGs as temperature sensor elements to realize a spatially distributed in-fiber temperature measurement during optical pumping. We study the temperature evolution in differently co-doped fibers under pumping conditions, identifying various effects contributing to the observed temperature increase.

2 Experimental Details

2.1 Fibers and Preparation

The investigated fibers were fabricated in-house by modified-chemical vapor deposition technology and solution doping. For our experiments, we chose fibers with comparable Yb₂O₃ concentrations around 0.35 mol. %. Our reference fiber is co-doped with 1.85 mol. % Al₂O₃, whereas our PD-reduced fibers are co-doped with cerium (Ce),¹⁹ with P/Al at ratio 1:1 and with much higher P₂O₅ content, respectively.²⁰ Detailed compositions of all fibers are given in Table 1. In addition, hydrogen loading of the reference fiber, which is known to decrease near-infrared (NIR)-PD as well,²¹ was performed before FBG inscription. In contrast,²² where H₂ loading was performed at high temperature that resulted in Yb²⁺ formation, our fiber was loaded at room temperature conditions. All the fibers employ a standard geometry with an 8- μ m core and a 125- μ m cladding diameter.

2.2 FBG Inscription and Characterization

A modified Talbot interferometer and UV fs pulses were used for FBG fabrication (for details see Ref. 12). The laser system consisting of a seed laser (Mantis, Coherent, Inc., Santa Clara, California), a regenerative amplifier (Legend Elite, Coherent), and a frequency tripler (HSG-T, Coherent) provides pulses of 266-nm wavelength, approximately 500-fs pulse duration, with a 1 kHz repetition rate. For FBG inscription, a power of approximately 300 mW was applied with a $1/e^2$ -beam diameter of approximately 6.3 mm, resulting in a maximum intensity in the focal region

of 320 GW/cm², where a cylindrical lens with a focal length of 390 mm was used to focus the laser pulse on the fiber.

For FBG fabrication, we chose a phase mask period of 1075 nm, resulting in a Bragg reflection wavelength near 1550 nm, to avoid any distortion of the Bragg reflected signal by pump light, amplified spontaneous emission (ASE) or PD-induced losses (NIR tail) of the Yb-doped fibers during temperature measurement. Furthermore, the fabricated FBGs show a medium reflectivity (<85%) to guarantee a proper peak measurement in reflection, as it is necessary for the applied measurement technique.

The temperature sensitivity of the FBGs was determined earlier to (10.9 ± 0.3) pm/K.²³ Because the fibers to be studied vary only slightly in doping concentrations, this temperature sensitivity was assumed for all fiber samples.

After grating inscription, the FBG possesses high losses, ranging from UV to NIR, that can be described as UV-induced PD in Refs. 18 and 23. Those losses disturb the proper sensor application of the FBG, because pump light will be absorbed causing a pronounced temperature enhancement due to UV-PD, which is not focus of this study. UV-PD can be removed by a temperature treatment²³ or photobleaching.¹⁸ The main advantage of a temperature treatment is that the absorbing species are annealed completely within just a few minutes when tempering the sample at about 550°C. But the disadvantage of this technique is a decreasing grating reflectivity, because the treatment affects not only the disturbing absorbing defects but also stress and compaction inducing defects, on which the index modulations defining the FBGs in case of fs pulse fabrication are mainly based. Utilizing a photobleaching treatment instead, the grating strength could be maintained due to the fact that only the disturbing color centers are affected. In addition, this technique is easily accessible and can be performed right after FBG inscription in the same setup using the same light source such as for FBG fabrication, just with lower average power. A detrimental influence is given by a residual absorbing defect concentration, which remains according to the model of equilibrium states of defects reported for NIR exposure²⁴ as well as UV.¹⁸ Nevertheless, by either of these treatments the disturbing broadband loss induced by the FBG fabrication can be removed.

2.3 Pump Experiments

To study the thermal behavior of Yb-doped fibers under pump load, core-pumping was performed. The core-pumping technique was preferred because the pump light is restricted to the fiber core and disturbances in the cladding area, i.e., through grating inscription and fiber fabrication, are negligible and do not affect the pump absorption or the temperature measurement. A sketch of the setup is given in Fig. 1. Pumping was performed using a commercial single-mode fiber coupled diode at 976 nm with 250 mW optical power. For analysis of the temperature behavior during pumping, only the part containing the FBG, approximately 1 cm fiber, was spliced between passive delivery fibers, ensuring a homogeneous inversion along this length. For the spatially resolved measurement, an FBG array of 10-cm length containing four FBGs was spliced between the delivery fibers. In that case, pump absorption changes over fiber length, thus an inhomogeneous temperature profile along the fiber arises. Experimental investigations on the

Table 1 Chemical fiber compositions.

Fiber	Yb ₂ O ₃ (mol. %)	Al ₂ O ₃ (mol. %)	Co-dopants (mol. %)
Reference fiber (1)	0.35	1.85	0
Ce co-doped fiber (2)	0.37	3.6	0.47 Ce ₂ O ₃ / 0.5 P ₂ O ₅
P/Al co-doped fiber (3)	0.3	3	3 P ₂ O ₅
high P co-doped fiber (4)	0.36	0	7.9 P ₂ O ₅
H ₂ loaded reference fiber (5)	0.35	1.85	(H ₂ loading)

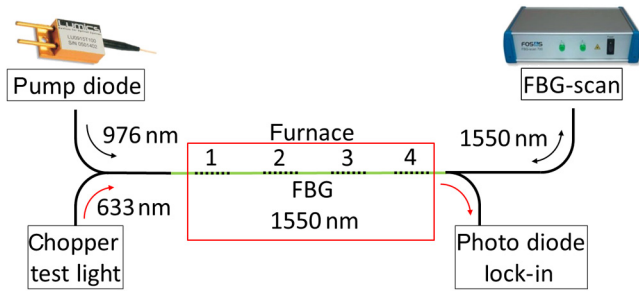


Fig. 1 Setup for spatially distributed temperature measurement via fiber Bragg grating (FBG) analysis, combined with near-infrared photodarkening (NIR-PD) measurement at 633 nm with a core-pumping at 976 nm. For proper analysis of thermal effects in PD-reduced fibers, only short fiber pieces containing one FBG were analyzed.

spatially distributed temperature evolution were restricted to a Ce-doped PD-reduced and the Yb/Al-doped reference fiber. The fibers can be moved into a tube furnace for thermal annealing of PD-induced defects.

To determine the temperature within the test fiber, we use an interrogator (FBGscan 608, FOS&S, Geel, Belgium) delivering test light around 1550 nm for the FBG wavelength monitoring and at the same time analyzing the Bragg wavelengths in reflection. From the wavelength shift of the FBG peak reflection, the temperature change within the fiber core can be estimated using the temperature sensitivity given above.

During pumping, it is also possible to monitor the PD loss at 633 nm, which is induced by the pump light itself (NIR-PD), using a chopper-lock-in technique as described earlier in Ref. 15. This measurement setup gives the possibility to correlate NIR-PD effects to the measured temperature changes.

3 Results and Discussion

3.1 Temperature and PD Measurements

Prior to the annealing of the reference fiber, the UV-induced PD causes a strong temperature increase of the FBG region during pumping. This is due to the UV-PD involving pump light absorbing defects. After removing the FBG inscription-induced losses by a temperature treatment as described before, the pumped FBG yields two distinguishable contributions to the temperature change as indicated in Fig. 2. An initial temperature step is assigned to an energy input through permanent loss of the fiber core, including the quantum defect (QD) that is the energy difference between pump and ASE light plus any additional absorption due to the background attenuation of the fiber. The second contribution is a dynamic loss, which increases during pumping. Comparing the temperature evolution to the NIR-PD measurement, we assign this effect to the growing absorption induced by pump light. This dynamic loss can be prevented, e.g., by appropriate co-doping of the Yb fibers (PD-reduced fibers, see Sec. 2.1).

3.2 Temperature Evolution in Differently Doped Fibers

In this section, we want to compare the temperature characteristics of differently co-doped fibers, i.e., our reference fiber and similar PD-reduced fibers (see Sec. 2.1). For proper comparison, all fibers containing an FBG have been

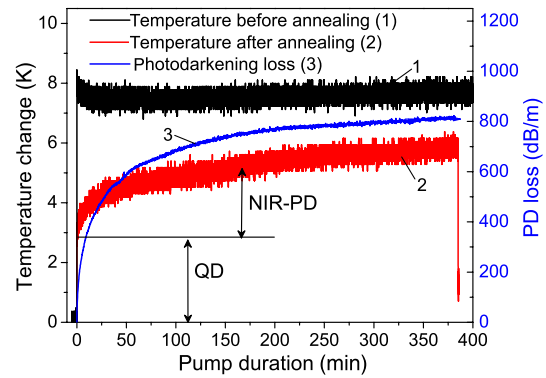


Fig. 2 Evolution of fiber temperature change and PD loss during pumping at 976 nm (reference fiber in water bath). The temperature increase before thermal treatment of the FBG is caused by UV-PD. After annealing of the UV-induced PD defects, only the quantum defect (QD) and subsequently induced NIR-PD contribute to the heating of the fiber core.

thermally treated to remove possible UV-PD before pumping. Temperature evolution of the pumped fibers is depicted in Fig. 3(a).

Although the Yb/Al-doped reference fiber shows an explicit dynamic temperature increase due to the NIR-PD, this effect is not observed for hydrogen loading of the same fiber prior to grating inscription. But in this particular case, the initial temperature step is dramatically increased. The reason for this performance is still under investigation. Changes in the valence state of the active ion may play an important role. Measured absorption spectra indicate the

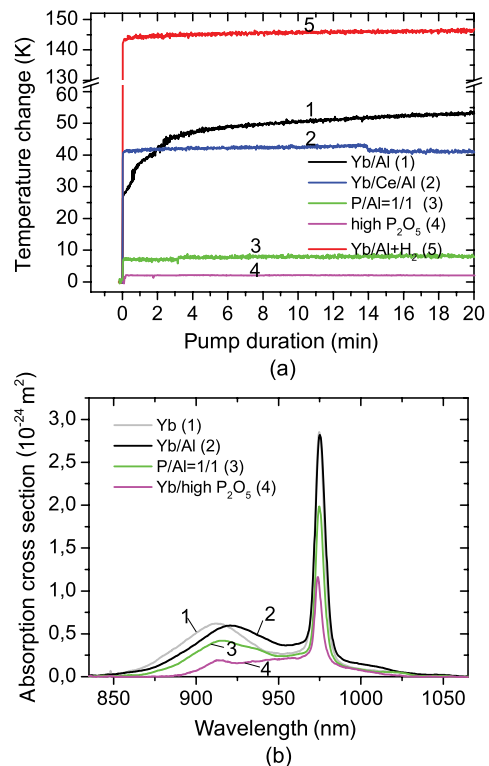


Fig. 3 (a) Temperature evolution during 976-nm pumping for differently doped, preannealed fibers measured utilizing an UV fs pulse inscribed FBG. (b) Absorption cross sections of differently co-doped Yb-doped fibers. Ce co-doping does not change the cross section significantly in comparison to Al co-doping.

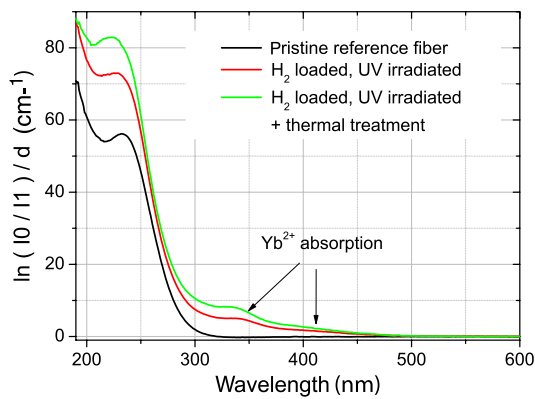


Fig. 4 Spectrum of pristine and hydrogen-loaded reference fiber showing Yb^{2+} absorption after UV irradiation and further on by subsequent thermal treatment.

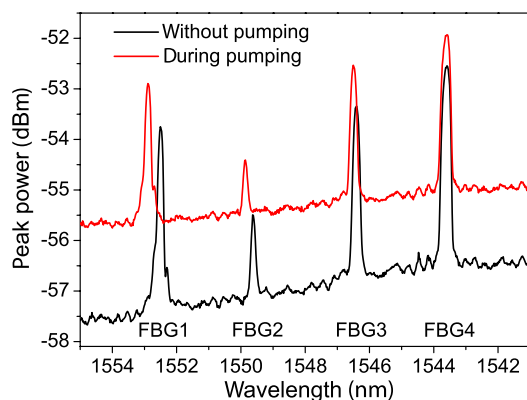


Fig. 5 Pumping of 10 cm Ce/Yb/Al-doped fiber containing four FBGs for temperature sensing. FBG 1 is situated next to the pump coupling, FBG 4 most distant. Different shifts of Bragg wavelength reflection peaks indicate an inhomogeneous temperature distribution along the fiber.

formation of Yb^{2+} by the exposure to UV radiation during FBG inscription for the hydrogen-loaded reference fiber (Fig. 4). This Yb^{2+} -formation through optical energy deposition is even reinforced by the following thermal treatment at 550°C .

The remaining PD-reduced fibers with Ce and P co-doping show also a negligible dynamic temperature increase during pumping. The initial temperature step at the beginning differs for the investigated fibers, although their Yb content is comparable. One reason for this behavior could be the difference in the Yb absorption cross sections, which directly influence the energy deposition through the QD, causing lower temperature shifts for $P/\text{Al} = 1/1$ and the highly P co-doped fiber [compare Fig. 3(b)]. The slightly larger temperature step of the Ce co-doped fiber cannot be explained by this effect and must have another origin, since the absorption cross section is not influenced by Ce co-doping.²⁵

3.3 Spatially Distributed Temperature Measurement

To demonstrate the applicability of the FBG temperature measurement in the spatial domain, we first fabricated an array of four FBGs within the Ce co-doped fiber, which is free of NIR-PD. During pumping, we observe different

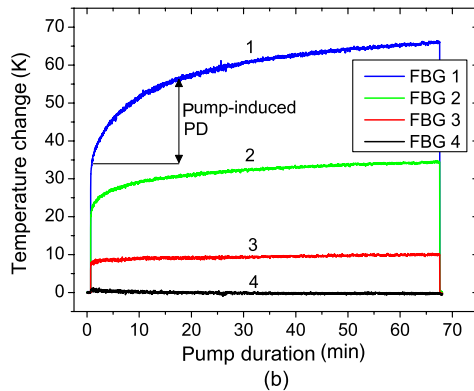
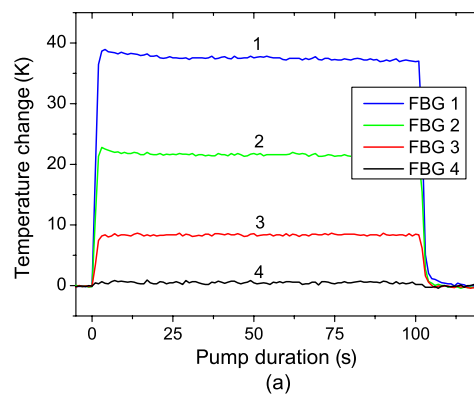


Fig. 6 Temperature evolution at different positions in 10-cm-long Yb fibers. The temperature step at the start of pumping is caused by the Yb absorption: (a) PD-reduced Ce-doped fiber and (b) reference fiber. NIR-PD occurs during pumping and causes an additional temperature increase.

but temporally constant changes of the Bragg wavelength, i.e., the fiber core temperature at different FBG positions in the fiber (Fig. 5). At the pump side (FBG 1), pump light is efficiently absorbed causing heating of the fiber due to permanent losses (QD). At the other side of the array, the available pump power decreases, resulting in a reduced absorbed power and inversion, and therefore in a lower temperature jump at the start of pumping. During pumping, only negligible changes in the dynamic loss, i.e., NIR-PD, occur [Fig. 6(a)].

To demonstrate the possibility of spatially distributed NIR-PD measurement, we repeated the same experiment on a 10-cm sample of our reference fiber. During pumping, we clearly observe the influence of the NIR-PD [Fig. 6(b)]. After the abrupt temperature step at the beginning of pumping, the temperature subsequently increases. This dynamic increase is more pronounced for FBG 1 than the other gratings because NIR-PD depends on the inversion, which is highest at the pump coupling side.

4 Conclusion

In this work, we developed a technique to investigate the in-core temperature dynamics in Yb-doped fibers during pumping. We clearly identified the main processes contributing to the temperature evolution. Although permanent losses due to the energy QD cause a sudden temperature change at the start of pumping in dependence on the Yb content, Yb inversion, and absorption cross section, an additional dynamic loss is obvious as subsequent temperature increase in Yb/Al-doped

fibers and almost negligible in PD-reduced fibers. Hydrogen loading of Yb/Al-doped fibers, which is known to reduce PD, seems to have a large impact on fiber temperature during optical pumping, probably supported by the absorption of UV-induced Yb^{2+} .

Utilizing a spatially distributed temperature measurement based on an FBG array, we find the core temperature to decrease with increasing distance from the pump coupling side, i.e., with decreased pump intensity. In the reference fiber, we additionally observe a temperature increase due to NIR-PD, which is also more pronounced by the higher pump power and inversion at the pump coupling side.

The presented measurement technique provides the new possibility to investigate the temperature profile in fiber lasers and amplifiers during operation and, if carefully calibrated, to determine the inversion profile. Derived from the established correlation of PD loss and induced temperature increase, the presented method is also well suited for spatially resolved PD measurements.

Acknowledgments

We gratefully acknowledge financial support by the Thuringian Ministry of Economics, Labor, and Technology (TMWAT) under contract 2011 FGR 0104 (FG Faser-Tech) with financial support from the European Social Fund (ESF).

References

1. D. J. Richardson, J. Nilsson, and W. A. Clarkson, "High power fiber lasers: current status and future perspectives," *J. Opt. Soc. Am. B* **27** (11), B63–B92 (2010).
2. K.O. Hill et al., "Photosensitivity in optical fiber waveguides: application to reflection fiber fabrication," *Appl. Phys. Lett.* **32**(10), 647–649 (1978).
3. G. Meltz, W. W. Morey, and W. H. Glenn, "Formation of Bragg gratings in optical fibers by a transverse holographic method," *Opt. Lett.* **14**(15), 823–825 (1989).
4. C. Chojetzki et al., "High-reflectivity draw-tower fiber Bragg gratings arrays and single gratings of type II," *Opt. Eng.* **44**(6), 060503 (2005).
5. L. Dong et al., "Efficient single-frequency fiber lasers with novel photosensitive Er/Yb optical fibers," *Opt. Lett.* **22**(10), 694–696 (1997).
6. J. T. Kringlebotn et al., " $\text{Er}^{3+}:\text{Yb}^{3+}$ -codoped fiber distributed-feedback laser," *Opt. Lett.* **19**(24), 2101–2103 (1994).
7. M. Ams et al., "Investigation of ultrafast laser-photonics material interactions: challenges for directly written glass photonics," *IEEE J. Sel. Top. Quantum Electron.* **14**(15), 1370–1381 (2008).
8. C. Smelser, S. Mihailov, and D. Grobnc, "Formation of type I-IR and type II-IR gratings with an ultrafast IR laser and a phase mask," *Opt. Express* **13**(14), 5377–5386 (2005).
9. D. N. Nikogosyan, "Multi-photon high-excitation-energy approach to fibre grating inscription," *Meas. Sci. Technol.* **18**(1), R1–R29 (2007).
10. E. Wikszak et al., "Erbium fiber laser based on intracore femtosecond-written fiber Bragg grating," *Opt. Lett.* **31**(16), 2390–2392 (2006).
11. M. Bernier et al., "Ytterbium fiber laser based on first-order fiber Bragg gratings written with 400 nm femtosecond pulses and a phase-mask," *Opt. Express* **17**(21), 18887–18893 (2009).
12. M. Becker et al., "Towards a monolithic fiber laser with deep UV femtosecond-induced fiber Bragg gratings," *Opt. Commun.* **284**(24), 5770–5773 (2011).
13. N. Jovanovic et al., "Stable high-power continuous-wave Yb^{3+} -doped silica fiber laser utilizing a point-by-point inscribed fiber Bragg grating," *Opt. Lett.* **32**(11), 1486–1488 (2007).
14. T. C. Newell et al., "Temperature effects on the emission properties of Yb-doped optical fibers," *Opt. Commun.* **273**(1), 256–259 (2007).
15. M. Leich et al., "Temperature influence on the photodarkening kinetics in Yb-doped silica fibers," *J. Opt. Soc. Am. B* **28**(1), 65–68 (2011).
16. M. L. Aslund et al., "Photodarkening study of gratings written into rare-earth doped optical fibres using a femtosecond laser," *Proc. SPIE* **6800**, 68000V (2008).
17. M. Leich et al., "In situ FBG inscription during fiber laser operation," *Opt. Lett.* **38**(5), 676–678 (2013).
18. J. Fiebrandt et al., "UV-induced photodarkening and photobleaching in UV-femtosecond-pulse-written fibre Bragg gratings," *Laser Phys. Lett.* **10**(8), 085102 (2013).
19. M. Engholm et al., "Improved photodarkening resistivity in ytterbium-doped fiber lasers by cerium codoping," *Opt. Lett.* **34**(8), 1285–1287 (2009).
20. S. Jetschke et al., "Efficient Yb laser fibers with low photodarkening by optimization of the core composition," *Opt. Express* **16**(20), 15540–15545 (2008).
21. J. Jasapara et al., "Effect of heat and H_2 gas on the photo-darkening of Yb³⁺ fibers," in *Conf. on Lasers and Electro-Optics/Quantum Electronics and Laser Science Conference and Photonic Applications Systems Technologies*, CTuQ5 (2006).
22. M. Engholm, L. Norin, and D. Åberg, "Strong UV absorption and visible luminescence in ytterbium-doped aluminosilicate glass under UV excitation," *Opt. Lett.* **32**(22), 3352–3354 (2007).
23. M. Leich et al., "Femtosecond pulse-induced fiber Bragg gratings for in-core temperature measurement in optically pumped Yb-doped silica fibers," *Opt. Commun.* **285**(21–22), 4387–4390 (2012).
24. S. Jetschke et al., "Photodarkening in Yb doped fibers: experimental evidence of equilibrium states depending on the pump power," *Opt. Express* **15**(22), 14838–14843 (2007).
25. S. Unger et al., "Optical properties of cerium-codoped high power laser fibers," *Proc. SPIE* **8621**, 862116 (2013).

Martin Leich received his DI in technical physics in 2007 from Technical University of Ilmenau, Germany. Since 2007, he has been employed as research scientist at the Leibniz Institute of Photonic Technology, Jena. He is skilled with fiber lasers, materials characterization of rare-earth-doped fibers, and the application of fiber Bragg gratings.

Julia Fiebrandt received her PhD in physics in 2014. She has been employed as junior scientist since 2011 at the Leibniz-Institute of Photonic Technology, Jena. Besides basic analysis of fiber Bragg gratings, their fabrication and properties and the application of the gratings as environmental sensors and in fiber lasers are the focus of her research.

Anka Schwuchow received her DI in communications engineering in 1994 from Technical University of Dresden. Since 1994, she has been employed as research scientist at the Leibniz-Institute of Photonic Technology, Jena. Her main research topics include the characterization of rare-earth-doped fibers and glass samples, pointing out their fluorescence properties and photodarkening issues.

Sylvia Jetschke received her PhD in physics in 1984 from Friedrich-Schiller-University, Jena. She is a senior scientist in the Leibniz-Institute of Photonic Technology, Jena. Since 1984, she has been engaged in the development and characterization of optical fibers for different applications. Her current research interests include photodarkening and related phenomena in Yb-doped laser fibers.

Sonja Unger works at the Leibniz-Institute of Photonic Technology as a research collaborator in the field of modified-chemical vapor deposition technology. She is engaged in research in the development of materials and high silica specialty optical fibers (active fibers for laser and amplifier, photosensitive fibers).

Matthias Jäger received his PhD in 1997 from the Center for Research and Education in Optics and Lasers (CREOL) at the University of Central Florida, before joining the Swiss Federal Institute of Technology ETH in Zurich (Switzerland) as a postdoctoral researcher. He is the head of the Active Fiber Modules group at the Leibniz Institute of Photonic Technology. From 2001 to 2011, he developed fiber lasers at ITF Optical Technologies in Montreal (Canada) and JT Optical Engine GmbH & Co. KG in Jena (Germany).

Manfred Rothhardt received his diploma degree in physics from Friedrich-Schiller-University, Jena, Germany, in 1984. He is a senior scientist in the Leibniz Institute of Photonic Technology, Jena. His current research interest includes applications of fiber Bragg gratings in sensors, biophotonics, and fiber lasers.

Hartmut Bartelt is a professor of modern optics at the University of Jena (Germany) and head of the Department of Fiber Optics in the Leibniz Institute of Photonic Technology. Research activities cover the fields of optical specialty fibers, micro- and nanostructured fiber optics, and fiber optical sensor elements.